RSC Advances

ROYAL SOCIETY OF CHEMISTRY

www.rsc.org/advances

Cite this: DOI: 10.1039/c0xx00000x

www.rsc.org/xxxxxx

ARTICLE TYPE

Peripheral functionalisation of a stable phthalocyanine J-type dimer to control the aggregation behaviour and NLO properties: UV–Vis, fluorescence, DFT, TDHF and thermal study

Alexander Yu. Tolbin, [*a] Alexander V. Dzuban,[b] Vladimir I. Shestov,[a] Yuliana I. Gudkova, [a] Valery K. Brel, [a,c] Larisa G. Tomilova, [a,b] and Nikolay S. Zefirov[a,b]

Received (in XXX, XXX) Xth XXXXXXXXX 20XX, Accepted Xth XXXXXXXXX 20XX
DOI: 10.1039/b000000x

This ~~novel~~ research opens the possibility of controlling the spectral, fluorescent and non-linear optical (NLO) properties of stable J-type phthalocyanine dimers. In our group, thermally and chemically stable supramolecular J-type dimers, based on low-symmetry phthalocyanine macrocycles, have been synthesised for the first time, and the present work is a fruitful continuation of initiated studies. Using an example of a dimeric magnesium complex, consisting of the same anti-parallel oriented 2-hydroxy-9,10,16,17,23,24-hexabutylphthalocyanine macrocycles, we first demonstrated the ability of stable phthalocyanine J-dimers to undergo peripheral functionalisation. UV–Vis, fluorescence and DFT studies showed that when 2-(diethylphosphoryl)-4-methylpenta-1,3-dienyl-3-oxy- moieties are introduced into a dimer structure, the intermolecular association of large molecules varies significantly, tending to ordering. Simulation of the nonlinear optical properties with the TDHF/6-311++G** theoretical approximation has shown that the chemical alteration of a dimeric structure results in an increasing polarisability (α), first hyperpolarisability (β) and an angle $\theta(\mu,\beta_{max})$ between the dipole moment μ and the main direction of the charge-transfer transition β_{max}.

Introduction

For a long time, phthalocyanines (Pcs), represented as macroheterocyclic compounds which are structurally related to naturally occurring porphyrins, have been used as traditional industrial dyes [1]. Significant expansion of Pcs applications has become possible due to the careful study of their physicochemical properties. Pcs can be used as optical recording materials, gas sensors, photosensitisers for photodynamic cancer therapy and in other promising areas [2]. Currently, phthalocyanine chemistry is developing intensively due to the study of such an important phenomenon as aggregation. It has been shown that low-symmetry phthalocyanines bearing various peripheral substituents may undergo self-assembly to form low stable J-aggregates in solutions [3-5]. Generally, J-type aggregation is caused by a slipped-cofacial configuration of chromophores [6] and was rarely observed among the phthalocyanine molecules until now. The J-type aggregates are very important in many applications such as optical data storage and NLO [7]. The presence of the polar substituents on the periphery of such compounds could reinforce valuable properties, in particular, due to the packing of the molecules in an material environment through hydrogen bonds [8]. Therefore, significant interest in the low-symmetry Pcs is given, which allows the fine-tuning of a substantial number of physical properties that enhance their technological advancements [9].

Recently, we have developed a simple preparative method for the synthesis of 2-hydroxyphthalocyanines [10]. The possibility of their use in the preparation of a wide range of covalently linked bi- and polycyclic *clamshell*-type phthalocyanines has also been shown [10-12]. In addition, we were the first to show that, in the presence of lithium methoxide and zinc acetate, 2-hydroxy-9(10),16(17),23(24)-tri-*tert*-butylphthalocyanine is able to produce a chemically- and thermally-stable *double-coordinated* dimeric complex, which was represented as a simple one-dimensional J-aggregate, or J-type phthalocyanine dimer [13, 14]. This important result gives rise to tremendous promise, since spectral and photophysical properties can be controlled simultaneously in two directions, namely, through the axial coordination of the various molecules and peripheral modification with the formation of nanoscale objects. Just recently, on an example of several low-symmetry monophthalocyanines, we have demonstrated that their modification by 2-diethoxyphosphoryl-4-methylpenta-2,3-dienyl methanesulphonate leads to a drastic change in the spectral properties [15]. In this work, we first demonstrate the possibility of peripheral modification of dodecabutyl-substituted stable J-type magnesium dimeric complex with this reagent to control aggregation and NLO properties.

Experimental

General methods

All solvents were reagent-grade quality and were obtained directly from Aldrich. Phthalocyanine ligand **1** was synthesized according to our previously published procedure [16]. UV–Vis spectra were recorded on a Hitachi U-2900 spectrophotometer in a range of 190–1100 nm in toluene and THF. FT–IR spectra were recorded in CCl_4 solution on a Nicolet Nexus IR-Furje spectrometer. ^{1}H NMR (500 MHz) spectra were recorded using a Bruker Avance III 500 MHz spectrometer. MALDI–TOF/TOF measurements were performed with a Bruker ULTRAFLEX II TOF/TOF spectrometer using 2,5-dihydroxybenzoic acid (DHB, Aldrich) and α-Cyano-4-hydroxycinnamic acid (HCCA, Aldrich) as a matrix. Thermogravimetric (TG) analysis was carried out on Netzsch STA 409 PC Luxx® thermal analyzer. Measurements were performed in alumina crucible (lid with hole) under an argon flow with a heating rate of 10°C/min up to 800°C. The fluorescence quantum yields (Φ_F) were estimated from fluorescence emission spectra (Varian Cary Eclipse Fluorescence Spectrophotometer) using PcZn in 1-propanol as a reference (λ_{ex} = 600 nm, Φ_F=0.45) [17]. Target-oriented approach was utilized for the optimization of the analytic measurements [18]. Before measurements the samples were mounted on a 25 mm aluminum specimen stub and fixed by conductive silver paint. Samples morphology was studied under native conditions to exclude metal coating surface effects [19]. The observations were carried out using Hitachi SU8000 field-emission scanning electron microscope (FE-SEM). Images were acquired in secondary electron mode at 0.7 kV accelerating voltage and at working distance 4-5 mm. Quantum-chemical calculations were performed with density functional theory (DFT) method. The Perdew–Burke–Ernzerhof (PBE) functional [20] and PRIRODA software package [21] supplied with cc-pVDZ basis set [22] were used for optimization of the structure geometries corresponded to steady state as well as for scanning of the potential energy surface (PES). Butyl substituents were replaced with hydrogen atoms for reducing a calculation time. *Ab initio* calculations of the static polarizability (α) and first hyperpolarizability (β) of complexes **2** and **4** have been carried out within the framework of the time-dependent Hartree-Fock method (TDHF). GAMESS (US) software package [23] and 6-311++G** basis set were used for evaluation of the ability of complexes **2** and **4** to exhibit NLO properties. All the quantum chemical calculations (gas-phase) were performed on an Intel/Linux cluster (Joint Supercomputer Center of Russian Academy of Scienses – www.jscc.ru). Visualization of the optimized structures and measuring of angles and distances were performed with Mercury program obtained from The Cambridge Crystallographic Data Centre (www.ccdc.cam.ac.uk).

Syntheses

Bis(2-hydroxy-9,10,16,17,23,24-hexabutylphthalocyanine [Mg]) (2). To a solution of **1** (430 mg, 0.49 mmol) in DCB (10 mL), CH_3OLi (90 mg, 2.37 mmol) was added followed by keeping of the mixture under reflux for 20 min. After that $Mg(CH_3COO)_2 \cdot 4H_2O$ (210 mg, 0.98 mmol) was added, and the mixture was refluxed for 30 min. After the reaction was finished (UV–Vis control), the residue was cooled to room temperature and treated with methanol (50 mL) followed by chromatographic purification of crude product on Bio-Beads SX-1 (THF as eluent). The title compound was obtained as a dark-blue solid (285 mg, 65%). ^{1}H NMR (DMSO-d_6): δ/ppm 9.80 (d, 2H, H^{α}, $^3J_{H-H}$ = 7.9Hz), 8.22 (d, 2H, H^{β}, $^3J_{H-H}$ = 8.1Hz); 9.38, 9.19, 9.08, 8.89, 8.58, 7.76, 7.59 (group of s, ∑=14H, $H^{\alpha'}$+H^{Ar}); 3.8–0.8 (m, 108H, Bu groups). FT-IR (CCl_4) ν (cm^{-1}): 3543–3094 (OH, valence vibrations), 2959–2863 (aromatic CH, valence vibrations), 1584–1335 (aromatic C–C, skeleton vibrations), 1069 (OH, skeleton vibrations), 751 (aromatic CH, deformation vibrations). MALDI–TOF/TOF (no matrix): m/z 1776.9122 ($[M-2H]^+$), calcd for $[C_{112}H_{128}Mg_2N_{16}O_2]$ 1778.9307. UV–Vis λ_{max} (nm) (log ε) in toluene: 350 (4.31), 688 (4.32), 764 (3.83); in THF: 350 (4.43), 629 (4.05), 678 (4.62), 702 (4.49). Fluorescence data: excitation λ_{max} (toluene) 600 nm, emission λ_{max} = 714 nm, Stokes' shift 26 nm, Φ_F=0.02; excitation λ_{max} (THF) 600 nm, emission λ_{max} = 704 nm, Stokes' shift 24 nm, Φ_F=0.06.

Bis(2-[2-(diethylphosphoryl)-4-methylpenta-1,3-dienyl-3-oxy]-9,10,16,17,23,24-hexabutylphthalocyanine [Mg]) (4)
To a solution of **2** (120 mg, 0.07 mmol) in toluene (1.5 mL), NaH (5 mg, 0.2 mmol) was added, and the mixture was ultrasonicated at 25°C for 15 min followed by addition of **3** [15] (55 mg, 0.18 mmol) dropwise. After 10 min the resulting solution was diluted with methanol (20 ml), and crude product was precipitated and filtered off. Target compound was purified on Bio-Beads SX-1 (eluent – THF) and Merck Silica gel 60 (gradient mixture – toluene/THF) to give a rosemary-tinted solid (90 mg, 58%). ^{31}P NMR (CCl_4): δ/ppm 18.1. ^{1}H NMR (CCl_4+5%DMSO-d_6): δ/ppm 9.7–10.3 (3d, 2H, H^{α}, $^3J_{H-H}$=8.0–8.2Hz), 8.2–8.5 ppm (3d, 2H, H^{β}, $^3J_{H-H}$=7.9–8.1Hz), 8.5–9.5 (group of s, ∑=12H, $H^{\alpha'}$+H^{Ar}), 6.16 (d, 2H, =CH_2, $^3J_{P-H}$(trans)=44.8Hz), 5.62 (d, 2H, =CH_2, $^3J_{P-H}$(cis)=21.4Hz), 3.7–0.5 (group of m, 144H, =C(CH_3), OEt, Bu groups). FT-IR (CCl_4) ν (cm^{-1}): 2954–2859 (aromatic CH, valence vibrations), 1597–1336 (aromatic C–C, skeleton vibrations), 1232 (C–O–C), 1092 and 1016 (P=O), 752 (aromatic CH, deformation vibrations). MALDI–TOF/TOF (matrix – DHB): m/z 2212.3967 ($[M+H]^+$), calcd for $[C_{132}H_{162}Mg_2N_{16}O_8P_2]$ 2211.3586. UV–Vis λ_{max} (nm) (log ε) in toluene: 354 (4.42), 631 (4.00), 684 (4.56), 712 (4.52); in THF: 351 (4.40), 625 (4.01), 678 (4.64), 703 (4.48). Fluorescence data: excitation λ_{max} (toluene) 600 nm, emission λ_{max} = 715 nm, Stokes' shift 29 nm, Φ_F=0.06; excitation λ_{max} (THF) 600 nm, emission λ_{max} = 682 nm, Stokes' shift 21 nm, Φ_F=0.06.

Results and discussion

Formation and structural characterisation

Optimisation of a previously proposed synthetic methodology [13], on the basis of ligand **1** [16], allowed us to obtain a stable magnesium dimeric complex of J-type (compound **2**) bearing on the periphery of 12 butyl groups and demonstrating the similar structural features and spectral properties. The modified approach consists of using of a non-polar environment (1,2-Dichlorobenzene – DCB) resulting in the production of dimeric complex **2** in a yield of 65%.

Cite this: DOI: 10.1039/c0xx00000x

www.rsc.org/xxxxxx

ARTICLE TYPE

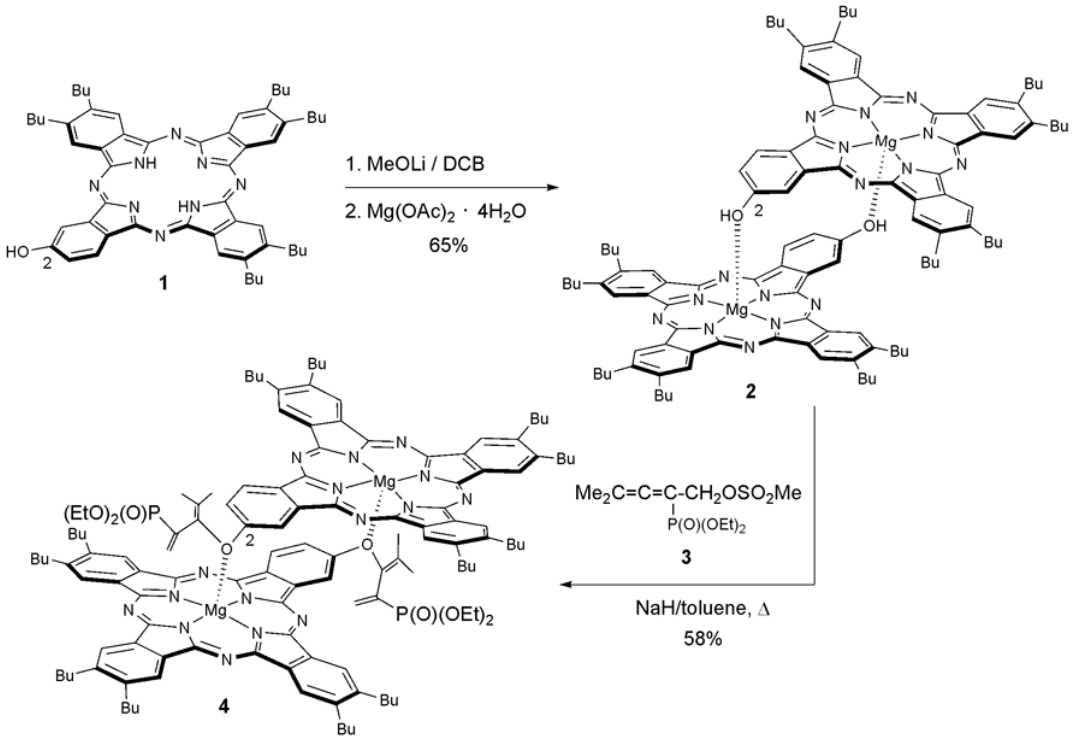

Scheme 1. Preparation of dodecabutyl-substituted J-type dimeric magnesium phthalocyanine complex **2** with subsequent structural modification in mild conditions to give the 2-[2-(diethylphosphoryl)-4-methylpenta-1,3-dienyl-3-oxy]-substituted derivative.

Increasing the symmetry of the structure and exclusion of the formation of regioisomeric products during the synthesis, as was in the case of the *tert*-butyl derivative [24], contributed to a significant improvement in the clarity of signals in the ^{1}H NMR spectrum that, along with the results of high-resolution mass spectrometry MALDI-TOF/TOF, led to reliable proof of the structure of the complex under study (Supporting information, Fig. S1-a). Thus, in the MALDI-TOF/TOF mass spectrum without a matrix, a single peak with m/z 1776.9122 ($[M–2H]^+$) with clear isotopic splitting was detected, which corresponds to a deprotonated molecular ion of complex **2**. Using matrixes such as 2,5-Dihydroxybenzoic acid (DHB) and α-Cyano-4-hydroxycinnamic acid (HCCA) enabled the observation of ion peaks with m/z 1930.9872 and 1966.0828 ($[M+DHB]^+$ and $[M–2H+HCCA]^+$ respectively) as well as the low-intensity ion peak with m/z 3555.8244 ($2\times[M–H]^+$). In the study of dimeric complex **2** with NMR spectroscopy, we observed a strong correlation of the proton spectrum with the nature of the solvent. It has been shown that the coordinating solvents, regardless of the concentration of a solution and temperature, led to a clear resolution of all signals. Thus, the signals of the aromatic protons of the phthalocyanine macrocycles were observed in the range of 7.5–10 ppm (DMSO-d_6). Proton signals H^{α} and H^{β} were detected as doublets at 9.80 and 8.22 ppm, respectively, with homonuclear vicinal constant of spin-spin coupling $^3J_{H–H}$ = 7.9Hz. The signals of proton $H^{\alpha'}$ and aromatic protons of isoindoline moieties containing butyl groups were represented as singlets which are observed in a broad range of 7.3–9.5 ppm, wherein the signals of the butyl groups were located in the region of 0.8–3.8 ppm (Supporting information, Fig. S2).

High stability of dimeric complex **2** allowed us to provide the nucleophilic reaction with 2-(diethoxyphosphoryl)-4-methylpenta-2,3-dienyl methanesulphonate (**3**) [15] to give complex **4** in 58% yield (Scheme 1). It should be noted that modification of the structure of a stable J-type dimer has been carried out for the first time, and the result is represented in the current study. During the synthesis, the destruction of dimeric molecules was not detected, and side reactions were mainly related to the processes of polymerisation in a strong basic medium with the participation of free multiple bonds (=CH_2). One of the features of the structure of dimer **4** is the almost complete fragmentation of the molecular ion in the absence of a matrix (MALDI–TOF/TOF). This was evidenced by the presence of high intensity peaks in the mass spectrum with m/z 1994.3155 ($[M–C_{10}H_{18}O_3P]^+$) and 1761.0732 ($[M–C_{10}H_{18}O_3P–C_{10}H_{18}O_4P]^+$). At the same time, butyl substituents were not subjected to fragmentation. Under mild ionisation conditions (matrix DHB), a single ion peak with m/z 2212.3967 ($[M+H]^+$) was observed, which corresponded to the molecular ion (Supporting information, Fig. S1-b). This result confirms the stability of

compound **4**, despite the presence of functional substituents on the periphery. The characteristic feature of 1,3-alkadienes-2-phosphonate is the presence in ^{1}H NMR spectrum of two doublets in the range of 5–7 ppm [25]. In our case, the doublets at 5.62 ppm ($^3J_{P-H(cis)}$=21.4Hz) and 6.16 ppm ($^3J_{P-H(trans)}$=44.8Hz) were responsible for the spin-spin interaction of phosphorus nuclei and protons of =CH_2 moieties, which reliably confirms the presence of (diethoxyphosphoryl)-alka-1,3-dienyl functional groups in the structure of complex **4** (Fig. 1).

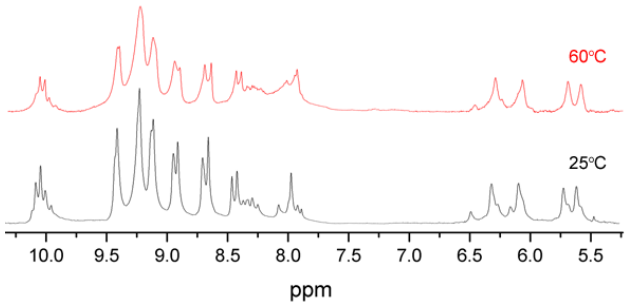

Fig.1. Partial ^{1}H NMR spectrum (CCl_4+5%DMSO-d_6) of complex **4** (C=3.65×10^{-4} mol dm^{-3}) at different temperatures. For details, see Supporting information (Fig. S3).

It was also shown that for 1,3-alkadienes-2-phosphonates, the transoid configuration [25] is more preferable, and is in excellent agreement with our results of theoretical modelling. Thus, scanning of the potential energy surface (PES) during changing the torsion angle Me_2**C**=**C**(OPc_2)–**C**(P(O)$(OEt)_2$)=**C**H_2 from 75° to 130° with a step of 3° allowed the observation of an energy barrier of 5.9 kcal/mol on the way of mutual transformation of possible Z- and E-isomers within the functional substituents of dimer **4**. Thus, the formation of transoid isomer (ΔE_{total} = –3.57 kcal/mol) is more likely. It should also be noted that there is a significant steric hindrance caused by phthalocyanine macrocycles. This makes the free rotation around the C–C bond in the diene moieties impossible, since the dimeric structure is rigid. For this reason, in the process of nucleophilic reaction, we cannot exclude the formation of several isomers (namely, inhibited rotamers), which differ from each other by the spatial orientation of the functional substituents and, possibly, some relative displacement of the phthalocyanine macrocycles in dimer **4**. This is confirmed by the NMR spectrum, in which several signals in the ranges of 9.7–10.3 and 8.2–8.5 ppm (H^{α} and H^{β}, respectively, doublets, $^3J_{H-H}$=7.9–8.2Hz) were observed, with a distorted waveform of the =CH_2 moieties. With increasing temperature, the smoothing of the =CH_2 signals occurred, confirming the partial rotation of alkadienyl phosphate moieties. Nevertheless, we assume that the mentioned isomers should not make a significant contribution to the changes in the spectral and optical properties of target dimeric complex **4**.

Thermal stability determination

Fig. 2 shows the results of thermal study of dimeric complexes **2** and **4**, which generally exhibit their high thermal stability in a solid state (450–480°C). This result is in agreement with our earlier data [14] and is caused by the specific structure of the dimers, in which the macrocycles are located at a distance of less than 3Å, allowing them to interact with each other via intermolecular forces of π–π-stacking. Such interactions are widely known for the majority of monophthalocyanines [26], but do not provide such incredible stability for macrocyclic aggregates. The reason for this is in a widely developed PES of interactions of the macrocycles and, according to our preliminary evaluation, searching of the global minimum on such surfaces is complicated by the reforming of spontaneously formed aggregates. The formation of coordination bonds between Mg ions and oxygen atoms of the OH-groups during the synthesis of complex **2** facilitates the fixing of the structure in the area of global minimum and leads to a stable dimeric molecule. This result is due to the feature of the synthetic method and was discussed in our previous work [24].

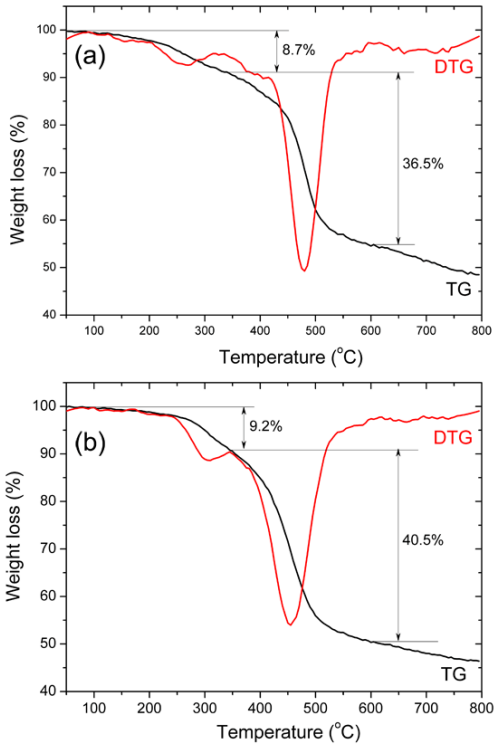

Fig. 2. TG and DTG curves for dimers **2** (a) and **4** (b).

Comparison of the thermoanalytical data for dimers **2** and **4** allows us to conclude that, in general, peripheral functionalisation does not significantly affect the stability of the dimeric complexes. As for the related *tert*-butyl zinc complex [14], decomposition of dimers **2** and **4** was observed within the temperature range of 250–500°C. This is evidenced by the low contribution of the volume of peripheral alkyl substituents and the nature of the complexing metal to the stability of the phthalocyanine dimers, since this stability is a result of the intramolecular π-π interactions between the macrocycles. The thermal destruction of complexes is almost the same. In the first stage, a partial thermal elimination of peripheral substituents was observed (weight loss of about 9%), followed by deeper fragmentation of the macrocyclic structures (weight loss of about 40%). At the same time, a bit higher stability of the 1,3-alkadienes-2-phosphonate substituents (compound **4**), compared to the butyl groups, may have been caused by the steric

hindrances during the thermal destruction. With increasing the temperature, a further degradation of the macrocycles occurred, which could not complete, even at 1000°C under an inert atmosphere.

Spectral properties and aggregation behaviour

The spectral properties of synthesised complexes **2** and **4** were close to those of previously obtained related compounds [13, 24]. Some features obtained by analytical studies indicate a tendency to intermolecular association of the dimeric molecules. In particular, the detection of ion peaks with double weight in the MALDI–TOF/TOF mass spectrum of dimer **2** suggests the dimerisation of charged molecules in a gas phase. At the same time, in the UV–Vis spectrum (toluene) in the range of 600–800 nm, a broadening of the absorption bands was observed (Fig. 3-a). Contrary, in the polar coordinating solvents (THF), the UV–Vis spectrum of complex **2** becomes typical of phthalocyanine J-type dimers [3, 13, 14], demonstrating a clearly resolved J-band which was red-shifted towards Q-band by 23–28 nm depending on the solvent nature.

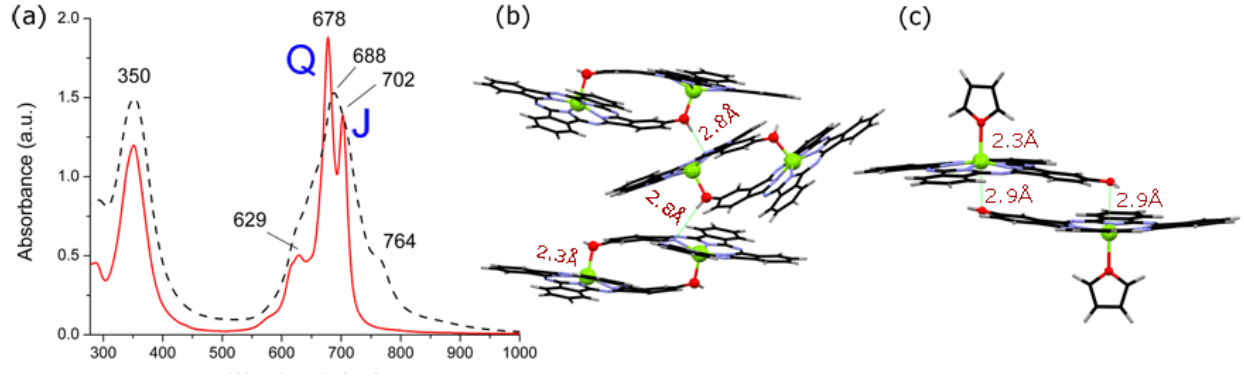

Fig.3. UV–Vis spectra (a) of complex **2** (C~6×10^{-5} mol dm^{-3}) in toluene (broken line) and THF (solid line) and assumed structure of aggregate (b) as an example of DFT-optimised structure of trimer based on **2**, which can be formed in non-coordinating solvents. Disaggregation in coordinating solvents is shown on a DFT-optimised model structure of **2**•2THF (c). Colour atoms coding: – hydrogen, – carbon, – nitrogen, – oxygen, – magnesium

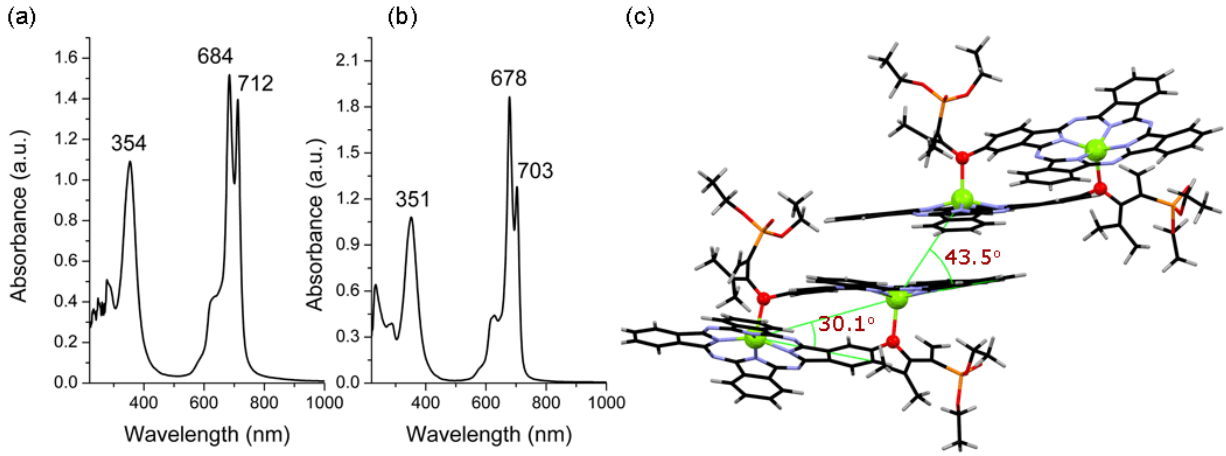

Fig 4. UV–Vis spectra of complex **4** (C~5×10^{-5} mol dm^{-3}) in toluene (a) and THF (b). The proposed association is presented on an example of DFT-optimised structure of dimeric J-aggregate which is composed of two molecules of complex **4** (c). Colour atoms coding: – hydrogen, – carbon, – nitrogen, – oxygen, – magnesium, – phosphorus.

The nature of the presented UV–Vis spectra was almost the same over a wide range of concentrations, up to 10^{-4} mol dm^{-3}. Aggregation is usually depicted as a coplanar association of macrocycles producing higher order structures and is attributed to the formation of π–π interactions between adjacent rings [27]. However, in our case, according to DFT-calculations, the aggregation of **2** in non-coordinating solvents may be due to the formation of intermolecular hydrogen bonds between the OH group of one molecule and the N_{iso} atom of a second (d(OH···N_{iso})=2.8Å). This assumption was confirmed by the FT–IR spectrum (Supporting information, Fig. S4), in which a broadened low-intensity band in the range of 3543-3094 cm^{-1} was found, corresponding to the stretching vibrations of OH groups and showing the presence of polyassociates fastened with hydrogen bonds. In coordinating solvents, disaggregation occurs by axial coordination of two solvent molecules by the complexing metal ions. At the same time, an increase in the slip angle of the macrocycles by Δθ = 11° was also observed with an enlargement of the Mg···O distance by 0.6Å. Fig. 3c and Fig. 4c showed a character of aggregation in toluene and disaggregation in THF. In the aggregated state, the structure of the complexed phthalocyanine rings was perturbed, resulting in the alternation of

the ground and excited state electronic structures [27]. This explains the experimental fact that, in nonpolar solvents, the fluorescence quantum yield of dimer **2** decreased several times compared with polar solvents (see Experimental section).

Aggregation can be controlled by the nature of substituents [28]. One can assume that the introduction of two bulky substituents into the structure of complex **2** will prevent the convergence of the dimeric molecules, strongly fix them in space and inhibit the formation of rigid aggregates. Recently, we have found that introduction into the phthalocyanine structure of the (diethoxyphosphoryl)-alka-1,3-dienyl functional groups leads to the formation of H- and J-type aggregates depending on the peripheral environment and the presence in the structure of the complexing metal [15]. Bulky substituents on the periphery of dimer **4** significantly alter the aggregation. This is evidenced by UV–Vis spectra of the complex, in which, independently of the solvent nature, there is a clear resolution of Q- and J-absorption bands with $\varepsilon \approx 32000$ L mol^{-1} cm^{-1} (Fig. 4-a,b). In the non-polar solvents (toluene), the J-band has a higher intensity that does not exclude the formation of more ordered associates than for the original complex **2**. As a consequence, there is a lack of correlation of the fluorescence quantum yield with the solvent nature; both in toluene and THF, Φ_F=0.06. According to DFT-calculations, the aggregation of dimeric complex **4** can only occur with the participation of π-π- stacking with the formation of J-aggregates (slip angle of 43.5°) constructed from J-type dimers (slip angle of 30.1°). In coordinating solvents, the dissociation of dimer **4** was not observed, which is caused by strong intramolecular interactions. It should also be noted that due to similarity of the UV–Vis spectra of dimeric complexes **2** and **4** in the most commonly used solvents, a different structure of dimer **4**, involving, in particular, coordination bonds P=O···Mg by analogy with [29], seems to be unlikely. In such case, according to the DFT-calculations, the distance between the macrocycles would be 5.4Å, which excludes π-π- interactions between them and reduces the stability of the macrocyclic compound. In other words, during the nucleophilic substitution (Scheme 2), the dimeric structure would undergo destruction to form corresponding monomeric product.

Introduction of the functional substituents to the structure of dimeric complex **2** does not significantly affect the value of the HOMO–LUMO gap ($\Delta E_g = E_{LUMO} - E_{HOMO}$=1.4 eV). However, aggregation decreases ΔE_g by 0.16 eV (when a trimer from **2** is formed, Fig. 3-c) and by 0.21 eV upon dimerisation of complex **4** (Fig. 4-c). This result is important for practical applications. Changing the nature of the central metal, along with a peripheral environment, together with the introduction of non-polar polymeric components into the composite structure will allow control of the electrical conductivity and nonlinear optical properties of organic materials based on stable J-type phthalocyanine dimers. We have also shown that aggregation is a beneficial process for such dimeric compounds. For the destruction of aggregates in a gas phase, according to the DFT-calculations, $\Delta E_{total} \approx 9$ kcal/mol of energy is required.

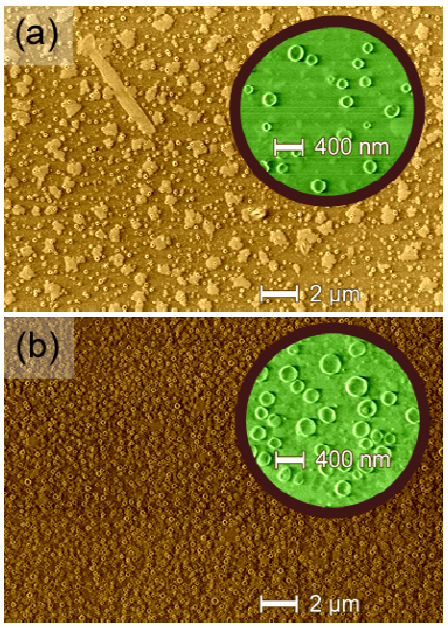

Fig. 5. FE-SEM images of dimeric complexes **2** (a) and **4** (b).

Aggregation of dimers **2** and **4** is also observed in the solid state. By means of field-emission scanning electron microscopy (FE-SEM), self-assembly of the dimeric molecules was found. As can be seen from Fig. 5, both complexes tend to the formation of rings with a diameter of 180–210 nanometres, and a wall thickness of about 30 nm, which corresponds to about 300 dimeric molecules packed in layers of about 20 molecules. This result is due to the specific structure of the dimeric complexes, in which the macrocycles are displaced from each other by an angle of about 30°. As a result of self-assembly, in accordance with the above-mentioned possible types of intermolecular association, the macromolecules undergo sequential shifting to form arcs which, with an increasing number of molecules participating in their formation, transform to closed circles. It is interesting to note that the original complex **2** was also characterised by the formation of irregular-shaped aggregates with a size ranging from 1.5 to 4 μm. Therefore, chemical modification of the J-type phthalocyanine dimeric complexes leads to disaggregation, which occurs both in solutions and in the solid state.

Fluorescence study

Fluorescence spectroscopy is a powerful tool for the study of electronic processes in phthalocyanines and related compounds. On the basis of fluorescence studies, the aggregation phenomenon, which depends both on the structure of macrocyclic compounds and the solvent nature, can also be investigated [27]. UV–Vis, fluorescence emission and excitation spectra of dimers **2** and **4** are shown in Fig. 6.

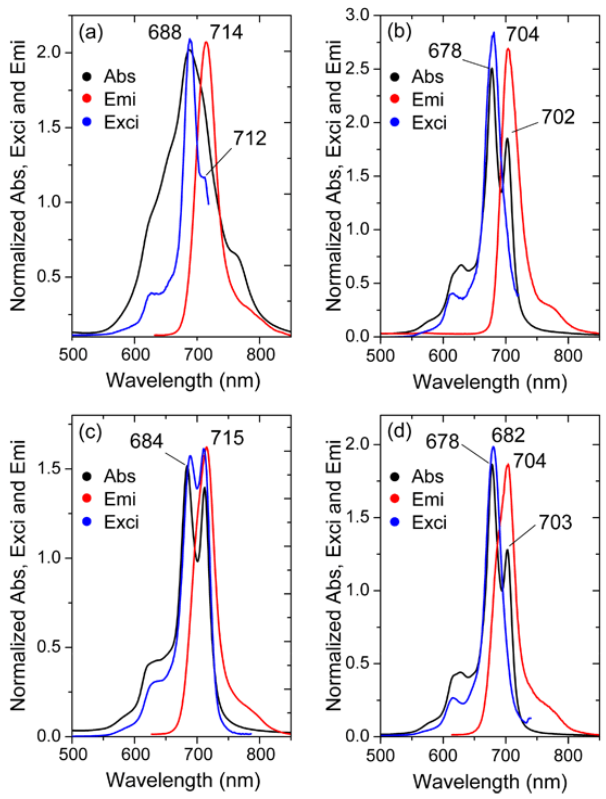

Fig. 6. UV–Vis absorption (Abs), excitation (Exci) and fluorescence emission (Emi) spectra of compounds **2** (a,b) and **4** (c,d) in toluene (a,c) and THF (b,d). See Supporting Information (Figs. S5–S8) for detail.

The results presented demonstrate the specific intermolecular association of complex **2** in a non-polar medium (Fig.6-a), as evidenced not only by a strong broadening of the Q-band in the UV–Vis spectrum, but also by a significant difference in the excitation and absorption spectra. In fact, the aggregation leads to fluorescence quenching, and in practice, for this compound, we observed a decrease in the fluorescence quantum yield in toluene by 3 times in comparison with THF. Introduction to the dimeric structure of bulky substituents (compound **4**) resulted in an ordering of dimeric molecules upon their association, giving rise to a similarity between the excitation and absorption spectra (Fig.6-c). Such an ordering, according to the simulation results, may be due to the formation of J-aggregates from the J-dimeric molecules, as shown in Fig. 4c. In THF, disaggregation was observed, which can be explained by the axial coordination of solvent molecules by ions of the complexing metal and is typical of both compounds. As a consequence, there is almost the same position of Q- and J-bands for both compounds in UV–Vis spectra (Fig. 3-a, 4-b, 6-b,d). The absence of the J-band in the excitation spectra should also be noted (Fig. 6-b,d). A similar phenomenon was observed for the related dimeric zinc complex in pyridine and explained by the fact that the axial coordination of the solvent leads to a weakening of the intramolecular contacts of the macrocycles in the dimer upon excitation, wherein the macrocycles are shifted with an increase in the slip angle [14]. However, this does not lead to dissociation of dimers **2** and **4**, since their ground spectra clearly demonstrate the J-band, which is characteristic of J-type dimers [5].

Time-dependent Hartree-Fock (TDHF) NLO properties

In the last decade, a lot of researchers have focused on the nonlinear optical (NLO) properties of organic materials due to their high potential in the production of photonic materials. Second-order NLO properties originate from the non-centrosymmetric alignment of chromophores and are widely known for phthalocyanines [26]. Polarisability (α) and the hyperpolarisabilities (β and γ) are important microscopic parameters of NLO materials, which characterise the response of a system in an applied electric field [30]. In this work, the evaluation and comparison of NLO properties of dimeric complexes **2** and **4** was performed on the basis of the TDHF/6-311++G** theoretical approach, which is considered to be a good compromise between accuracy and calculation duration [31], and is suitable for phthalocyanines [32]. Total static dipole moment μ, isotropic polarisability α, the polarisability anisotropy $\Delta\alpha$, the mean first polarisability β, the angle $\theta(\mu,\beta_{max})$ (deg.) between the dipole moment μ and the main direction of the charge-transfer transition β_{max} were calculated according to equations 1–5 using the x, y, z tensor components from the GAMESS output. The calculation results are given in Table 1.

$$\mu = \left(\sum_{i=x,y,z} \mu_{ii}^2 \right)^{1/2}$$

$$\alpha = \tfrac{1}{3} \sum_{i=x,y,z} \alpha_{ii}$$

$$\Delta\alpha = 2^{-1/2} \left[(\alpha_{xx} - \alpha_{yy})^2 + (\alpha_{yy} - \alpha_{zz})^2 + (\alpha_{zz} - \alpha_{xx})^2 \right]^{1/2}$$

$$\beta = \left(\beta_x^2 + \beta_y^2 + \beta_x^2 \right)^{1/2}, \text{ with } \beta_x = \beta_{xxx} + \beta_{xyy} + \beta_{xzz};$$

$$\beta_y = \beta_{yyy} + \beta_{yzz} + \beta_{yxx}; \ \beta_z = \beta_{zzz} + \beta_{zxx} + \beta_{zyy}$$

$$\theta(\mu, \beta_{\max}) = \arccos \left(\frac{\left| \sum_i \mu_i \beta_i \right|}{\left(\sum_i \mu_i^2 \times \sum_i \beta_i^2 \right)^{1/2}} \right),$$

where i=x,y,z

As can be seen, the polarisabilities (α) of the dimeric molecules differ from each other by 11%, while the first hyperpolarisability (β) of the peripherally functionalised dimer **4** is much larger (1.5 times) than that of **2**. Starting complex **2** had the largest polarisability anisotropy (232.3 Å^3), which can be attributed to the lower compactness of this compound. An important parameter for acentric alignment degree for the first hyperpolarisabilities is angle $\theta(\mu,\beta_{max})$ between the direction of the permanent dipole moment μ and the main direction of the first hyperpolarisability β_{max} [31]. For dimer **4**, we observed magnification of the dipole moment (1.6 times) and the angle $\theta(\mu,\beta_{max})$ (almost 3 times), which is a consequence of increasing the asymmetry of the electronic density. This result explains the enhancement of the second-order nonlinearity of dimer **4** and causes a reduction of the probability of antiparallel arrangement of first hyperpolarisabilities in bulk materials [33]; therefore, the peripheral modifications of stable phthalocyanine J-type dimers may prove promising for second-order nonlinear optical applications.

Cite this: DOI: 10.1039/c0xx00000x

www.rsc.org/xxxxxx

ARTICLE TYPE

Table 1. Results of the TDHF/6-311++G** calculations: static dipole moments, μ(D), isotropic polarizabilities (α), anisotropy of polarizabilities ($\Delta\alpha$), zero-frequency mean first hyperpolarizabilities, β (esu) and the angle $\theta(\mu,\beta_{max})$ (deg.).

Compound[a]	μ(D)	α(Å^3)[b]	$\Delta\alpha$ (Å^3)[b]	β ($\times10^{-30}$ esu)[b]	$\theta(\mu,\beta_{max})$, (deg.)
2	2.68	127.4	232.3	39.77	11.7
4	4.44	143.8	226.9	60.95	33.2

[a] The calculations were performed on the models of compounds **2** and **4**, in which butyl groups were replaced by hydrogen atoms to reduce a calculation time.

[b] Since the values of the polarizability (α) and the hyperpolarizability (β) of the GAMESS output are reported in atomic units (a.u.), the calculated values have been converted into Å^3 for α and $\Delta\alpha$ (1 a.u. = 0.14817 Å^3) and into electrostatic units (esu) for β (1 a.u. = 8.639×10^{-33} esu).

Conclusions

In this work, the first example of modification of the structure of a stable phthalocyanine J-type dimer was presented with emphasis placed on controlling aggregation, as well as spectral and NLO properties. The thermoanalytical study has demonstrated the high thermal stability of the dimeric compounds up to 480°C. Field-emission scanning electron microscopy revealed the ability of dimeric complexes to form rings with an average diameter of about 200 nm. Chemical modification of the J-type phthalocyanine dimeric complexes did not decrease their stability, but only led to disaggregation, which occurred both in solution and in the solid state. Implementation of the time-dependent Hartree-Fock approach allowed us to estimate the NLO properties of synthesised compounds, wherein the higher hyperpolarisability of complex **4** can be explained by the presence in the structure of the (diethoxyphosphoryl)-alka-1,3-dienyl functional moieties, which can withdraw the electronic density from phthalocyanine rings. Therefore, molecules of complex **4** possess a push-pull structure, where charge transfer can arise from the π–conjugated macrocyclic system to the functional substituents. The high molecular asymmetry of **4** caused a large angle $\theta(\mu,\beta_{max})$, suggesting the affection of peripheral functional substitutes to the optical second-order nonlinearity.

Acknowledgements

The research was supported by Council under the President of the Russian Federation for State Support of Young Scientists and Leading Scientific Schools (Grant MK-6590.2013.3) and the UFC of MSU under financial support of the Ministry of Education and Science of Russian Federation (Contract N16.552.11.7081). The authors also thank Joint Supercomputer Center of RAS (www.jscc.ru) for providing computing resources. Electron microscopy characterization was performed in the Department of Structural Studies of Zelinsky Institute of Organic Chemistry, Moscow. The authors acknowledge partial support from the M.V. Lomonosov Moscow State University Program of Development.

Notes and references

[a] Institute of Physiologically Active Compounds, Russian Academy of Sciences, 142432 Chernogolovka, Moscow Region (Russian Federation)

[b] Department of Chemistry M. V. Lomonosov Moscow State University, 119991 Moscow (Russian Federation)

[c] A.N.Nesmeyanov Institute of Organoelement Compounds, Russian Academy of Sciences, 119991, GSP-1, Moscow, V-334, Vavilova St. 28, INEOS (Russian Federation)

† Electronic Supplementary Information (ESI) available: characterization and theoretical calculations. See DOI: 10.1039/b000000x/

‡ Corresponding author. Tel.: +7 496 5242566, e-mail address: tolbin@ipac.ac.ru (Dr. A.Yu. Tolbin).

1. P. Erk, H. Hengelsberg, *in: K.M. Kadish, K.M. Smith, R. Guilard (Eds.), The Porphyrin Handbook, vol. 19, Academic Press, San Diego, 2003, p. 105*.
2. A.Yu. Tolbin, A.V. Ivanov, L.G. Tomilova, N.S. Zefirov, *J. Porphyrins Phthalocyanines*, 2003, **7**, 162-166.
3. K. Kameyama, M. Morisue, A. Satake, Y. Kobuke, *Angew. Chem. Int. Ed.*, 2005, **44**, 4763-4766.
4. X. Huang, F. Zhao, Z. Li, L. Huang, Y. Tang, F. Zhang, C.-H. Tung, *Chem. Lett.*, 2007, **36**, 108-109.
5. V. Novakova, P. Zimcik, K. Kopecky, M. Miletin, J. Kunes, K. Lang, *Eur. J. Org. Chem.*, 2008, **19**, 3260-3263.
6. M. Morisue, S. Ueda, M. Kurasawa, M. Naito, Y.Kuroda, *J. Phys. Chem. A*, 2012, **116**, 5139−5144.
7. M. Sevim, M.N. Yaraşir, A. Koca, M. Kandaz, *Dyes and Pigments*, 2014, **111**, 190-201.
8. D. Asthana, R. Pandey, and P. Mukhopadhyay, *Chem. Commun.*, 2013, **49**, 451-453.
9. M.S. Rodríguez-Morgade, G. de la Torre, T. Torres, *in: K.M. Kadish, K.M. Smith, R. Guilard (Eds.), The Porphyrin Handbook, vol. 15, Academic Press, New York, 2003 (Chapter 99)*.
10. A.Yu. Tolbin, Victor E. Pushkarev, L.G. Tomilova, and N.S. Zefirov, *Mendeleev Commun.*, 2009, **19**, 78-80.
11. A.Yu. Tolbin, V.E. Pushkarev, G.F. Nikitin, and L.G. Tomilova, *Tetrahedron Lett.*, 2009, **50**, 4848-4850.
12. A.Yu. Tolbin, V.E. Pushkarev, L.G. Tomilova, *J. Porphyrins Phthalocyanines*, 2012, **16**, 341-350.
13. A.Yu. Tolbin, V.E. Pushkarev, I.O. Balashova, L.G. Tomilova, *Mendeleev Commun.*, 2013, **23**, 137-139.

14. A.Yu. Tolbin, V.E. Pushkarev, I.O. Balashova, A.V. Dzuban, P.A. Tarakanov, S.A. Trashin, L.G. Tomilova, N.S. Zefirov, *New J. Chem.*, 2014, **38**, 5825-5831.
15. A.Yu. Tolbin, V.E. Pushkarev, I.O. Balashova, V.K. Brel, Yu.I. Gudkova, V.I. Shestov, L.G. Tomilova, *J. Porphyrins Phthalocyanines*, 2013, **17**, 343-350.
16. V.E. Pushkarev, A.Yu. Tolbin, N.E. Borisova, S.A. Trashin, and L.G. Tomilova, *Eur. J. Inorg. Chem.*, 2010, **33**, 5254-5262.
17. A.T. Gradyushko, A.N. Sevchenko, K.N. Solovyov, M.P. Tsvirko, *Photochemistry and Photobiology*, 1970, **11**, 387-400.
18. V.V. Kachala, L.L. Khemchyan, A.S. Kashin, N.V. Orlov, A.A. Grachev, S.S. Zalesskiy, V.P. Ananikov, *Russ. Chem. rev.*, 2013, **82**, 648–685.
19. A.S. Kashin, V. P. Ananikov, *Russ. Chem. Bull. Int. Ed.*, 2011, **60**, 2602-2607.
20. M. Erznzerhof, G.E. Scuseria, *J. Chem. Phys.*, 1999, **110**, 5029.
21. D. N. Laikov, Yu. A. Ustynyuk, *Russ. Chem. Bull., Int. Ed.*, 2005, **54**, 820-826.
22. D.N. Laikov, *Chem. Phys. Lett.*, 2005, **416**, 116-120.
23. M.W. Schmidt, K.K. Baldridge, J.A. Boatz, S.T. Elbert, M.S. Gordon, J.H. Jensen, S. Koseki, N. Matsunaga, K.A. Nguyen, S. Su, T.L. Windus, M.Dupuis, J.A. Montgomery, *J. Comput. Chem.*, 1993, **14**, 1347–1363.
24. A.Yu. Tolbin, V.E. Pushkarev, V.B. Sheinin, S.A. Shabunin, L.G. Tomilova, *J. Porphyrins Phthalocyanines*, 2014, **18**, 155-161.
25. V.K. Brel, A.V. Dogadina, B.I. Ionin, A.A. Petrov, *Russ. J. Gen. Chem.*, 1982, **52**, 520-524.
26. H.S. Nalwa, ed., *Supramolecular Photosensitive and Electroactive Materials*, Academic Press, San Diego, 2001.
27. T. Nyokong, E. Antunes, *Photochemical and Photophysical Properties of Metallophthalocyanines, in the Handbook of Porphyrin Science (eds. K.M. Kadish, K.M. Smith, R. Guilard), World Scientific Press*, 2010, **7**, 247-357.
28. W. Chidawanyika, T. Nyokong, *Photochem. Photobiol. A: Chemistry*, 2009, **206**, 169-176.
29. F. Atefi, J.C. McMurtrie, D.P. Arnold *Dalton trans.*, 2007, **48**, 2163-2170.
30. O. Christiansen, J. Gauss, J.F. Stanton, *Chem. Phys. Lett.*, 1999, **305**, 147-155.
31. O-P. Kwon, M. Jazbinsek, J.-In Seo, P.-J. Kim, E.-Y. Choi, Y. S. Lee, P. Günter, *Dyes and Pigm.*, 2010, **85**, 162-170.
32. A. Zawadzka, A. Karakas, P. Plociennik, J. Szatkowski, Z. Łukasiak, A. Kapceoglu, Y. Ceylan, B. Sahraoui, *Dyes and Pigm.*, 2015, **112**, 116-126.
33. S.-J. Kwon, O.-P. Kwon, J.-In Seo, M. Jazbinsek, L. Mutter, V. Gramlich, Y.-S. Lee, H. Yun, P. Günter, *J. Phys. Chem. C*, 2008, **112**, 7846–7852.